Food Chemistry 460 (2024) 140574

Contents lists available at ScienceDirect

Food Chemistry

journal homepage: www.elsevier.com/locate/foodchem

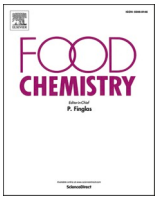

Ice recrystallization inhibition activity of pulse protein hydrolysates after immobilized metal affinity separation

Joshua Saad [a], Murillo Longo Martins [b], Vermont Dia [a,*], Toni Wang [a,*]

[a] Department of Food Science, The University of Tennessee, 2510 River Dr, Knoxville, TN 37996-4539, USA
[b] Institute for Advanced Materials and Manufacturing, The University of Tennessee, 2641 Osprey Vista Way, Knoxville, TN 37920, USA

ARTICLE INFO

Keywords:
Ice recrystallization inhibition
Immobilized metal affinity chromatography
Pulse proteins
Protein hydrolysates

ABSTRACT

Creating molecules capable of inhibiting ice recrystallization is an active research area aiming to improve the freeze-thaw characteristics of foods and biomedical materials. Peptide mixtures have shown promise in preventing freezing-induced damage, but less is known about the relationship between their amino acid compositions and ice recrystallization inhibition (IRI) activities. In this article, we used Ni^{2+} immobilized metal affinity chromatography (IMAC) to fractionate pulse protein hydrolysates, created by Alcalase and trypsin, into mixtures lacking and enriched in His, and Cys residues. The aim of this study was to fractionate pulse protein hydrolysates based on their amino acid compositions and evaluate their resulting physicochemical and IRI characteristics. Ni^{2+} IMAC fractionation induced IRI activity in all of the evaluated soy, chickpea, and pea protein hydrolysates regardless of their amino acid composition. Ni^{2+} IMAC fractionation produced chemically distinct fractions of peptides, differing by their molecular weights, amino acid composition, and IRI activities. The resulting peptide mixtures' molecular weight, amino acid composition, secondary structure, and sodium ion levels were found to have no correlation with their IRI activities. Thus, we demonstrate for the first time the ability of Ni^{2+} IMAC fractionation to induce IRI activity in hydrolyzed pulse proteins.

1. Introduction

The recrystallization of ice can damage foods and biomedical materials, often affecting their sensory characteristics and bioactivity (Zhang et al., 2023). Commonly exacerbated by temperature fluctuations during storage and transportation, the recrystallization of small ice crystals to larger crystals can cause damage to cells by puncturing membranes and increasing osmotic stress, affecting the quality and functionality of the frozen product (Zhang et al., 2023). Thus, the creation and subsequent implementation of ice recrystallization inhibiting molecules is an active research area aiming to improve the freeze-thaw characteristics of food products and the survival rate of cells (Biggs et al., 2019; Tian, Zhu, & Sun, 2020). While ice recrystallization inhibition (IRI) agents occur naturally, such as anti-freeze proteins (AFPs) and glycoproteins, their minuscule concentration and costly extraction have led to efforts to create bio-based mimetics from sources such as food proteins and carbohydrates (Li, Zhao, Zhong, & Wu, 2019; Voets, 2017). Pulses are of great interest for this application because of their abundant globulin storage proteins such as vicilins (7S) and legumins (11S), with well-documented food safety, and scalable production quantity.

Additionally, a multitude of bio-based and synthetic molecules have been found to possess IRI activity, including varieties of protein and other structures including non-hydrolyzed proteins, peptide mixtures and single amino acids, synthetic and bio-based dyes, carbohydrates, synthetic polymers, etc. (Biggs et al., 2019; Warren, Galpin, Bachtiger, Gibson, & Sosso, 2022). Resulting from their individual and diverse molecular features, several mechanisms have been proposed for these compounds' IRI activities. Regarding proteins, previous studies have shown relationships between IRI activity and numerous molecular characteristics, including but not limited to molecular weight, amphiphilicity, secondary structure, and amino acid composition, making the characterization of molecules important in understanding IRI activity (Biggs et al., 2019; Zhang et al., 2022). Specifically, the amino acid composition of proteins has been suggested to play a role in their IRI activities. A previous study performing structural and functional modeling of AFPs found that seven AFPs were highly hydrophobic and lacked three amino acids specifically, cysteine, histidine, and tryptophan (Bhattacharya et al., 2018). Additionally, it was found that in preparation of enzymatically hydrolyzed collagen, that the amino acid composition of the active fraction lacked tryptophan and cysteine,

* Corresponding authors.
E-mail addresses: vdia@utk.edu (V. Dia), twang46@utk.edu (T. Wang).

https://doi.org/10.1016/j.foodchem.2024.140574
Received 3 April 2024; Received in revised form 25 June 2024; Accepted 21 July 2024
Available online 29 July 2024

possessing only a small amount of histidine (Cao et al., 2020). Thus the manipulation and removal of particular amino acids such as tryptophan, cysteine, and histidine, may result in peptide products with increased IRI activities.

Immobilized metal affinity chromatography (IMAC) can separate peptide mixtures based on their ability to form coordination complexes with immobilized metal ions, dependent on amino acid composition and peptide structure (Porath, 1988). Particularly, histidine, tryptophan, and cysteine residues can form coordination complexes with metal ions (Porath, 1992). These coordination complexes are formed because of transition metal ions' ability to act as Lewis acids, accepting lone pair electrons from atoms such as oxygen, nitrogen, and sulfur (Holmes & Schiller, 1997). Additionally, different metal ions possess unique affinities to different atoms dependent on the Pearson system that categorizes metal ions as hard, intermediate, and soft based on their reactivity toward nucleophiles (Porath, 1988). Hard metal ions prefer oxygen, intermediate ions nitrogen, oxygen, and sulfur, while highly polarizable soft metal ions prefer sulfur (Porath, 1988). Ions such as Fe^{3+} and Ca^{2+} are categorized as hard metal ions and used for specialized fractionation such as calcium binding peptides or phosphopeptides (Holmes & Schiller, 1997; Lv, Bao, Liu, Ren, & Guo, 2013). Ni^{2+} and Co^{2+} are more suitable to complex a diverse group of proteins and peptides, such as hydrolyzed food proteins (Gutiérrez, Martín del Valle, & Galán, 2007; Porath, 1992).

Thus, we hypothesize that separating peptide mixtures according to their ability to form coordination complexes (isolation based on His, Cys) with Ni^{2+} immobilized metal ions will create peptide fractions with enhanced IRI activity, resulting from the imitation of amino acid compositions identified from studied IRI peptides and proteins. Further, we hypothesize that IMAC fractionation of hydrolyzed pulse proteins into bound (enriched in His, Cys) and unbound fractions (lacking His, Cys) will result in a bound fraction lacking IRI activity, and an unbound fraction with enhanced IRI activity. In this article, we for the first time implement Ni^{2+} IMAC fractionation to study the relationship between peptide amino acid compositions and their IRI activity, separating peptide mixtures by their His and Cys residues. Additionally, we evaluate the ability of Ni^{2+} IMAC fractionation to create anti-freeze materials from non-IRI active food sources, evaluating a new IRI agent creation strategy. The aim of this study was to fractionate pulse protein hydrolysates based on their amino acid compositions and evaluate their resulting physicochemical and IRI activities.

2. Materials and methods

2.1. Materials

Soy protein isolate (13.3% carbohydrate, 0% fat, 83.3% protein) and pea protein (0% carbohydrate, 8.7% fat, 70% protein) were purchased from bulk supplements.com (Henderson, NV). Chickpea protein (3.1% carbohydrate, 4.7% fat, 78.1% protein) was purchased from Green Boy Group (Los Angeles, CA). Alcalase was purchased from Millipore Sigma (Burlington, MA) and trypsin was purchased from Alfa Aesar (Ward Hill, MA) and used at 0.176 Au/g and 280 Au/g, respectively.

2.2. Enzymatic hydrolysis of pulse protein isolates

Soy, chickpea, and pea protein isolates were hydrolyzed by Alcalase and trypsin. Briefly, a 10% dispersion of the protein isolates was suspended in deionized (DI) water and the pH was adjusted to optimum conditions (both at pH 8) using a NaOH solution. The dispersions were then placed in a shaking water bath under optimum temperatures for each enzyme (Alcalase 55 °C and trypsin 37 °C) and allowed to equilibrate for 15 min. The enzyme was then added (Alcalase at 0.176 Au/g and trypsin at 280 Au/g). The trypsin hydrolysis time was 2 h for the soy isolate and 4 h for the pea and chickpea isolates. The Alcalase hydrolysis time was 10 min for all the protein isolates. Different hydrolysis times were selected to create a proper range of molecular weight distributions for the subsequent IMAC treatment. The samples were then placed in a boiling water bath for 10 min to denature the proteases, and centrifuged at 20,000*g*, 15 min, 4 °C. The supernatant was then separated from the residue and lyophilized to produce a powder used for all subsequent treatments.

2.3. Ni^{2+} IMAC fractionation of the protein hydrolysates

An iminodiacetic acid (IDA) IMAC column was created by packing a glass buret with layers of fiberglass, silicon dioxide, and 10 mL of IDA Chelating Sepharose Fast Flow purchased from Cytiva (Marlborough, MA). Modified from a previous study (Lin et al., 2021) to fractionate the samples, the column was first drained of 20% ethanol used for storage and the resin was washed with 5 column volumes (CV) of DI water, followed by 3 CV of 0.2 M nickel (ii) sulfate hexahydrate. Then, an additional 2 CV of 0.2 M nickel (ii) sulfate hexahydrate was added to the resin and incubated for 30 min. After incubation, 5 CV of DI water was passed through the column followed by 5 CV of the elution buffer (0.05 M Na_3PO_4, 0.5 M NaCl, pH 4) to remove loosely bound metal ions. Following, 5 CV of equilibrating buffer (0.05 M Na_3PO_4, 0.5 M NaCl, pH 7.4) was passed through the column to equilibrate the resin for fractionation. Approximately 40 mg of the hydrolysate samples were added to 1 mL of equilibrating buffer, vortexed, and added to the column. Then, 3 CV of equilibrating buffer was passed through the column, collected, and labeled the "unbound fraction" followed by 3 CV of eluting buffer collected and labeled the "bound fraction". The fractionation of the samples into the "unbound" and "bound" fractions was determined by monitoring the pH of the eluent. The bound fraction was collected when the pH of the eluent decreased from 7.4. After the bound fraction was collected, 3 CV of equilibrating buffer was used to wash the column to prepare for the next fractionation. Following, another 40 mg of the same hydrolysate sample was added into the column and the procedure was repeated 2 more times for a total of 3 fractionations per sample (~120 mg per isolate sample). The metal ions were eluted (using 0.2 M EDTA) and recharged for different protein hydrolysate sample fractionations. After the final fractionation, the column was washed with 5 CV of DI water and stored in 2 CV of 20% (*v*/v) ethanol.

2.4. Dialysis and lyophilization of IMAC fractions

Before dialysis, the IMAC fractionated pulse hydrolysates were partially lyophilized to reduce sample volume. To desalt the IMAC fractions, SnakeSkin™ dialysis tubing with a cut-off of 3.5 kDa was used (Thermo Fischer Scientific, Waltman MA). Dialysis tubing was cut and presoaked in DI water before use. The fractions were added to the dialysis tubing and placed in approximately 200x – 500x the sample volume of DI water, changing the water every 2 h, 4 times a day, after which the samples were stored overnight at 4 °C. Water changes and overnight storage were repeated for a total of 4 days and upon completion, the samples were placed in pre-weighed 50 mL centrifuge tubes. These samples were lyophilized until a fine powder was obtained and used for all sample characterizations.

2.5. Quantification of remaining sodium ions in IMAC samples after dialysis

Briefly, lyophilized IMAC fractions were solubilized in 1× PBS to achieve a concentration of 2% (*w*/*v*) and allowed to stand at room temperature (RT) to achieve temperature equilibrium. All other solutions measured were allowed to stand until RT. A Horiba Na-11 Laquatwin Sodium Ion (Na^+) Meter (Kyoto, Japan) was calibrated using 150 ppm and 2000 ppm NaCl solutions. Once calibrated, solutions containing known quantities of sodium ions (1× PBS, 10 mM NaCl, 100 mM NaCl) were quantified by placing 300 μL of each solution on the sensor. Similarly, the IMAC fractions were quantified by placing 300 μL

of solution on the sensor. To calculate the final Na^+ concentration, the ppm quantity of sodium measured was converted to mM Na^+ using the following formula:

((Avg.IMAC fraction (in PBS) sodium ion ppm–PBS sodium ion ppm)/(22.99))
= IMAC sample sodium ion mM conc.(*22.99 represents the molecular weight of sodium ions*)

2.6. IMAC fraction molecular weight distribution measured by size exclusion chromatography-high performance liquid chromatography (SEC-HPLC)

The IMAC fractions with a concentration of 20 mg/mL (in PBS) were diluted with HPLC-grade water to achieve a concentration of 1 mg/mL. The sample was then filtered through a 0.45 μm PTFE chromatography syringe filter and added to 2 mL autosampler HPLC vials for SEC-HPLC. The fractions were analyzed by SEC-HPLC using an Agilent 1200 HPLC system for 20 min as previously described (Saad & Dia, 2023). Briefly, samples were separated using a BioSep-SEC-S2000 column (300 × 7.80 mm, Torrance, CA) with a mobile phase containing 45% acetonitrile and 0.1% trifluoroacetic acid in water, with a flow rate of 1.0 mL/min, an injection volume of 20 μL. Samples ran for 20 min at ambient temperature and were detected at a wavelength of 214 nm. The average molecular weight was calculated using standard curve created from a mixture of proteins and peptides with known molecular weights containing albumin (66,000 Da), aprotinin (6500 Da), glucagon (3482 Da), bradykinin acetate (1060 Da), bradykinin fragment 1–5 (573 Da), L-glutathione (307 Da), and glycine (75 Da).

2.7. Quantification of the IMAC fraction amino acid composition

Using a modified method from a previous work (Akhlaghi, Ghaffari, Attar, & Alamir Hoor, 2015), 50 μL of the 20 mg/mL IMAC fractions suspended in 1× PBS was added into specific hydrolysis tubes and combined with 1.1 mL of 6 M HCl. The hydrolysis tube was then sealed under vacuum and placed in a pre-heated block at 150 °C for 30 min. After hydrolysis, the samples were cooled to room temperature, and the vacuum in the tubes was released. The samples were then placed into a vacuum oven pre-heated between 50 and 60 °C under vacuum to dry overnight. The dried sample was combined with 1 mL of 50 mM $NaHCO_3$ pH 8.4 sample buffer and vortexed until dissolved. Following, 50 μL and 25 μL of the dissolved sample were combined with 150 μL and 175 μL of 50 mM $NaHCO_3$ pH 8.4 sample buffer to create 2 dilutions with total volumes equaling 200 μL. These samples were then combined with 300 μL of 4-(Dimethylamino)azobenzene-4′-sulfonyl chloride solution (1.3 mg/mL acetonitrile) and vortexed for 30 s. The samples were then heated at 70 °C for 20 min, shaken periodically (5 and 15 min), and placed in an ice bath to stop the reaction. Following, 500 μL of diluent solution was added (50 mM sodium phosphate buffer of pH 7 and HPLC grade ethanol at 1:1), vortexed, and filtered with a 0.45 μm nylon filter for HPLC analysis. The samples were analyzed by HPLC, performed on a Zorbax Eclipse Plus C18 (4.6 × 250 mm) column with a mobile phase containing 25 mM sodium acetate (pH 6.5) and 4% dimethyl formamide, at a flow rate of 1.0 mL/min, an injection volume of 10 μL, maintained at 40 °C, and detected at a wavelength of 436 nm. The samples were injected alongside a serial dilution of an amino acid standard mixture (Sigma, AA-S-18) prepared using the same methods as the samples.

2.8. Splat assay and ice crystal quantification

A standard splat assay procedure was used to analyze IRI activity (Knight, Hallett, & DeVries, 1988). The assay was performed using a variety of analyte concentrations in 1× PBS buffer; with the same concentration (*v*/v) of PEG in 1× PBS buffer serving as the control. One drop (~10 μL) was dropped from a 1.5-m height onto a precooled (−80 °C) microscope slide. The slide was annealed at −8 °C using a cryo-stage HCS 302 (Instec Instruments, Boulder, CO) for 30 min, with pictures taken using light microscopy (Leica, DM2700 M, Wetzlar, Germany) after 30 min. Quantification of ice crystals was performed using Cellpose and Fiji using the Feret's maximum diameter and standard deviation to measure ice crystal size (Saad, Fomich, Día, & Wang, 2023).

2.9. Secondary structure analysis by Raman spectroscopy

The secondary structure of the protein hydrolysates and IMAC fractionated samples were evaluated by Raman spectroscopy. Briefly, samples at a 2% concentration in 1× PBS were added dropwise into an aluminum pan for evaluation. The measurement was conducted using a Horiba T64000 spectrometer equipped with a DXR green laser (532 nm). Data was collected with an acquisition time of 5 s and an accumulation of 180 s. The data were processed in OriginPro (ver. 10.05) by baseline subtraction and decomposition of the spectral region of interest (amide I) in Voigt curves (an example of the fit spectra can be seen in Supplementary Fig. 2) (Bradley, n.d.). The secondary structures of the samples were calculated using the area under the curve of the Voigt fit curves after spectral decomposition.

2.10. Statistical analysis

All treatments were repeated in duplicate or triplicate. Correlation analysis of the various molecular characteristics and IRI was performed in JMP Pro ver. 17.0.0.

3. Results and discussion

3.1. Preparation and characterization of pulse protein hydrolysates and their IRI activities

3.1.1. Enzyme hydrolysis and MW profile

Soy, chickpea, and pea hydrolysates were prepared by Alcalase and trypsin hydrolysis. Enzyme hydrolysis was performed to create peptide mixtures with varying physicochemical properties that are different from their protein's isolates, as numerous studies have reported improved IRI activity from protein isolates upon hydrolysis (Cao et al., 2020; Cao et al., 2023; Fomich et al., 2023; Zhang et al., 2022). This improvement in IRI activity is attributed to favorable peptide size compatibilities with the ice lattice, cooperative effects among peptides when present at an interface, changes in H-bonding abilities, and increased amphiphilicity (Cao et al., 2020; Cao et al., 2023; Fomich et al., 2023; Zhang et al., 2022). Alcalase is a nonspecific endopeptidase while trypsin is an endopeptidase selective for the C-terminal side of lysine and arginine, resulting in the creation of differing peptide compositions between the enzyme treatments (Tacias-Pascacio et al., 2020; Vajda & Szabó, 1976). Lastly, soy, chickpea, and pea protein isolates were hydrolyzed by Alcalase for 10 min to create relatively small

Table 1
Molecular weight profiles and IRI activities of pulse protein isolates (2%) before and after hydrolysis.

Sample	Molecular weight (kDa), %					Feret Diameter of Ice (%PEG)
	≥50	10–49.9	5–9.9	1–4.9	≤ 1	
SPI	27.5 ± 0.5	23.6 ± 0.1	9.3 ± 0.3	18.9 ± 0.1	20.8 ± 0.2	114.1 ± 8.7[a]
CPI	54.9 ± 8.5	24.0 ± 9.6	9.1 ± 2.7	3.8 ± 1.1	8.2 ± 0.5	120.5 ± 2.2[a]
PPI	58.8 ± 0.6	24.4 ± 0.5	0.0 ± 0.0	5.7 ± 0.1	11.1 ± 0.0	131.6 ± 13.2[a]
Try SPH	21.6 ± 5.3	27.1 ± 2.7	6.6 ± 2.9	15.3 ± 1.2	29.3 ± 9.7	103.7 ± 0.5[a]
Try CPH	0.0 ± 0.0	47.5 ± 0.4	24.0 ± 0.3	16.2 ± 0.0	12.2 ± 0.1	108.6 ± 0.2[a]
Try PPH	0.0 ± 0.0	5.9 ± 0.3	0.0 ± 0.0	75.2 ± 0.2	18.8 ± 0.1	118.4 ± 2.1[a]
Alc SPH	0.0 ± 0.0	9.7 ± 5.3	5.0 ± 0.1	28.3 ± 1.7	55.7 ± 3.4	112.1 ± 2.1[a]
Alc CPH	2.6 ± 0.5	1.0 ± 0.5	7.3 ± 2.1	32.4 ± 1.2	56.7 ± 0.2	106.0 ± 0.1[a]
Alc PPH	0.0 ± 0.0	0.0 ± 0.1	4.5 ± 2.4	35.8 ± 7.5	59.6 ± 0.3	105.0 ± 3.0[a]

SPI, CPI, and PPI represent the soy, chickpea, and pea protein isolates before hydrolysis, respectively. Try and Alc represent the trypsin and Alcalase enzymes used to hydrolyze the protein isolates, respectively. SPH, CPH, and PPH represent the soy, chickpea, and pea protein hydrolysates, respectively. The Feret diameter value is the percent ice crystal size relative to the PEG control. Thus, 100% would indicate that the ice crystal size induced by the sample was the same size as the IRI inactive PEG control. [a]Means followed by different letter(s) within the same column are significantly different from each other ($P < 0.05$, $n = 2$).

peptide sizes, while soy was hydrolyzed by trypsin for 2 h and pea and chickpea were hydrolyzed by trypsin for 4 h to achieve a larger average molecular weights than the Alcalase treatments.

Upon enzyme hydrolysis, the mass distribution (Supplementary Table 1) of protein hydrolysates into the supernatant and residue fractions varied among the samples and enzyme treatments. The recovery of the protein hydrolysates into the supernatant fractions ranged from 44.5% to 76.4%. The supernatant fraction was used for the remainder of the study, as the IMAC treatment requires soluble material to successfully fractionate the peptides by their respective amino acid.

Characterization of the pulse protein material molecular weight profiles was achieved by SEC-HPLC to determine the effect of hydrolysis on their molecular weight distributions. As shown in Table 1, the Alcalase and trypsin hydrolysis greatly affected the molecular weight distribution of the pulse protein hydrolysates. Prior to hydrolysis the soy, chickpea, and pea protein isolates possessed 39.7%, 12.0%, and 16.8% of their molecular weight fraction between <1–5 kDa, respectively. After hydrolysis, the Alcalase hydrolyzed pulses showed a greatly reduced molecular weight distribution of 84.0%, 89.1%, and 95.4% of the hydrolysate molecular weight between <1–5 kDa for the soy, chickpea, and pea hydrolysates, respectively. These modified molecular weight distributions indicate the successful hydrolysis of the pulse protein isolates by Alcalase that created a mixture of small molecular weight peptides. Similarly, the pulse proteins hydrolyzed by trypsin showed a change in their molecular weight distributions after hydrolysis. Distinct from the Alcalase hydrolysates, the trypsin hydrolyzed pulse proteins showed a broader molecular weight distribution range, containing a higher percentage of the larger peptides with sizes ranging from 5 to 50 kDa. While the trypsin hydrolysis preserved a higher percentage of larger peptides when compared to the Alcalase treatment, the trypsin hydrolysis was still effective in reducing the molecular weight distribution of the starting protein isolates, creating a broader molecular weight distribution with weights ranging from >50–1 kDa. This difference in the endpoint molecular weight distribution can be attributed to the differences in the enzyme's specificity and treatment times. Thus, Alcalase and trypsin were both successful in hydrolyzing the soy, chickpea, and pea protein isolates, creating various peptide mixtures with different molecular weight distributions for evaluation in the subsequent IMAC fractionation.

3.1.2. IRI activity

The IRI activities of the pulse proteins hydrolysates before IMAC treatment were evaluated to determine if the hydrolysis treatments promoted IRI activity from the newly created peptide mixtures. Shown in Table 1, at a 2% peptide concentration, the hydrolysis treatment did not promote IRI activity for either the Alcalase or trypsin hydrolysates relative to the PEG control. Interestingly, our Alcalase soy hydrolysate did not promote IRI activity in comparison to work done by Fomich and coworkers whose soy Alcalase hydrolysate produced potent IRI activity upon 10-min hydrolysis (Fomich et al., 2023). Although they used a similar concentration of analyte to our study, the random specificity of Alcalase enzyme may affect the final composition of peptides produced after hydrolysis. Furthermore, differences in the soy protein isolate source and processing conditions may also affect the IRI activities of the hydrolyzed product. Regardless, our pulse protein hydrolysates possessing no IRI activity were then fractionated by Ni^{2+} IMAC to evaluate the fractionation treatment effect of their IRI activities.

3.2. Fractionation of pulse proteins hydrolysates by Ni^{2+} IMAC and their IRI activities

3.2.1. Preparation of Ni^{2+} IMAC fractionated pulse hydrolysates

The pulse protein hydrolysates were fractionated using Ni^{2+} IMAC to create peptide mixtures enriched (bound fraction) or lacking (unbound fraction) cystine, histidine, and tryptophan. After fractionation, dialysis and lyophilization were performed to remove excess salt (NaCl, Na_3PO_4) from the IMAC fractions, as these salts have been previously reported to affect IRI activities and the crystallization behavior of ice in the splat assay (Surís-Valls & Voets, 2019a). Because dialysis is not selective for salt alone, also removing low MW peptide material, we created additional samples to control for the treatment effect of dialysis on IRI activity to ensure the loss of low MW peptides would not affect our determination of the relationship between key amino acid residues and IRI activity. Thus, we created the "hydrolysate dialysis" sample and the

Table 2
Mass recovery of the trial 1 and 2 protein hydrolysates after fractionation, dialysis, and lyophilization.

Sample	Unbound Mass (%)	Bound Mass (%)	Total Recovery (%)
Alc Soy	61.1	38.9	49.5
Try Soy	61.7	38.3	82.7
Alc Chickpea	63.6	36.4	56.2
Try Chickpea	54.2	45.8	59.4
Alc Pea	76.6	23.4	48.6
Try Pea	69.4	30.6	43.3
Alc Chickpea T1	63.6	36.4	56.2
Alc Pea T1	76.6	23.4	48.6
Try Soy T1	61.7	38.3	82.7
Alc Chickpea T2	69.8	30.2	52.9
Alc Pea T2	67.4	32.6	59.7
Try Soy T2	60.7	39.3	64.8

The top portion of the table displays the mass recovery of the pulse hydrolysates after the preliminary IMAC fractionation. The bottom portion of the table displays the mass recovery of the selected pulse hydrolysates used for the remainder of the study after preliminary IMAC fractionation. T1 represents trial 1, T2 represents trial 2. Both trials describe replicate IMAC, dialysis and lyophilization treatments. The mass recovery (%) of peptides in the unbound and bound fractions is relative to the total recovery. The total recovery is relative to the starting mass of the peptides introduced into the IMAC column before fractionation, dialysis, and lyophilization.

"combination" sample. The "hydrolysate dialysis" sample was created to evaluate the effect of dialysis on the hydrolysate IRI activity independent from the Ni^{2+} IMAC fractionation. This sample was used to determine if the removal of low MW peptides contributed to changes in IRI activity. The mass recovery of the hydrolysate dialysis samples was 23.3% for Alc chickpea, 21.1% for Alc pea, and 67.4% for try soy. Furthermore, we evaluated a "combination sample" which is the combination of the unbound (UB) and bound (B) fractions after IMAC fractionation. The sample ID "combo" indicates that the sample was hydrolyzed by either Alcalase or trypsin and was fractionated by Ni^{2+} IMAC. After fractionation, the UB and B fractions were re-combined before dialysis and lyophilization. The mass recovery of the combination samples was 49.9% for the Alc chickpea, 59.6% for the Alc pea, and 90.2% for try soy, displaying similar values to the total recovery of the hydrolysates fractionated into the UB and B fractions in Table 2.

3.2.2. *Mass distribution of pulse hydrolysates after Ni^{2+} IMAC fractionation*

The mass distribution of the pulse protein material into the B and UB fractions after IMAC fractionation is shown in Table 2. Other recorded fractionation conditions such as flow rate can be seen in the supplemental information (**Supplementary Table 2**). As expected, the mass recovery of peptides into the UB fraction was consistently higher than the B fraction, likely because of the relatively low abundance of amino acid residues implicated in binding with immobilized metal ions. Furthermore, the mass recovery of the UB and B samples were affected by sample loss during dialysis, lowering the overall mass recovery of both the UB and B fractions. Interestingly, the ratio of mass recovered in the UB:B fractions shows close similarities among all the pulse protein hydrolysates displaying a ~ 2:1 mass recovery ratio between the UB and B fractions. While the abundance of histidine, cysteine, and tryptophan residues on the peptides is relatively low, the ~30% total recovery for the B fractions is likely due to chaperon proteins; the protein-protein interaction that occurs between the immobilized metal ion, metal binding cluster (MBC) on the peptide (the placement of His, Cys and Trp) and proteins bound to the peptide containing the MBC (Lingg et al., 2020). The amino acid composition of these fractions will be discussed later.

3.2.3. *Splat assay screening of pulse hydrolysates after Ni^{2+} IMAC fractionation*

After fractionation, dialysis, and lyophilization, the fractionated pulse hydrolysates were evaluated for their IRI activities by the splat assay. As shown in Table 3, all the hydrolyzed pulse protein samples that were fractionated and dialyzed displayed IRI activity relative to the PEG control. IRI activity varied between samples displaying mean ice crystal FD ranging from 57.5 ± 4.4% to 82.8 ± 2.7% relative to the size of the PEG control. Interestingly, our hypothesis that B fractions enriched in His and Cys would not possess IRI activity was not observed. It is possible that the IMAC fractionation resulted in peptide mixtures in both B and UB fractions with the ability to cooperatively occupy the ice water interface that results in the inhibition of ice recrystallization. This could alter the ability of the peptide mixtures to orient themselves at the ice-water interface resulting in IRI. For instance, antifreeze peptides from shark collagen hydrolysates were prepared using different chromatographic techniques (Wang, Zhao, Chen, Zhou, & Wu, 2014). In this study, a combination of charge, size, and hydrophobic affinity separations were used to enhance the hypothermic protective activity of shark collagen hydrolysates resulting in increased antifreeze activity from 12.4% to 88.9% (Wang et al., 2014). Our IMAC technique on the other hand showed the ability to create both fractions with enhance IRI activity when compared to its starting material. Because of the large number of samples and numerous subsequent characterization techniques utilized, we chose to continue to investigate 3 samples specifically, chickpea hydrolyzed by Alcalase, pea hydrolyzed by Alcalase, and soy hydrolyzed by trypsin. Chickpea and pea hydrolyzed by Alcalase were chosen over trypsin chickpea and pea because of their high IRI activity and better solubility facilitated by Alcalase hydrolysis. Further, the trypsin hydrolyzed soy sample was chosen for subsequent characterization due to its large molecular weight distribution when compared to the Alcalase hydrolyzed samples allowing a more diverse set of samples to be characterized.

Table 3
The IRI activities of the Ni^{2+} IMAC fractionated pulse protein hydrolysates (2%).

Sample	Enzyme Treatment	IMAC Fraction	Feret Diameter (%PEG)
Soy	Alcalase	Unbound	70.6 ± 2.3^{abc}
		Bound	64.4 ± 3.2^{bc}
	Trypsin	Unbound	72.3 ± 4.6^{ab}
		Bound	65.5 ± 1.5^{bc}
Chickpea	Alcalase	Unbound	66.2 ± 2.2^{bc}
		Bound	57.5 ± 4.4^{c}
	Trypsin	Unbound	72.2 ± 0.9^{ab}
		Bound	81.9 ± 2.1^{a}
Pea	Alcalase	Unbound	59.1 ± 2.9^{bc}
		Bound	82.8 ± 2.7^{a}
	Trypsin	Unbound	73.1 ± 1.1^{ab}
		Bound	61.3 ± 0.2^{bc}

The Feret diameter value is the percent ice crystal size relative to the PEG control. Thus, 100% would indicate that the ice crystal size induced by the sample was the same size as the IRI inactive PEG control. The standard deviation is the variation of crystal size (%) between duplicate splat assay measurements. [a]Means followed by different letter(s) within the same column are significantly different from each other ($P < 0.05$, $n = 2$).

3.2.4. *Mass distribution of trials 1 and 2 Alc chickpea, Alc pea, and try soy Ni^{2+} IMAC fractions*

To confirm our initial observations gained from the screening of the IMAC fractionated pulse hydrolysates, the selected samples were fractionated again in duplicate (named trial 1 and 2). As seen earlier in Table 2, when comparing the percent recovery of the hydrolysates between the trial 1 and 2 treatments, similar percent values were obtained aside from the Alcalase chickpea sample whose percentage of trial 1 mass was altered due to a spill during sample processing. This indicates that the removal of low MW material during dialysis was similar between the two trials and that the subdivision of peptides during IMAC was consentient when evaluating the mass percentage recovered in the UB and B fractions. Further, the trypsin soy hydrolysate showed consistently higher recovery than the Alcalase hydrolyzed chickpea and pea hydrolysates. This is likely due to the enzyme treatment creating more peptides >3.5 kDa (the dialysis membrane cut-off) allowing more peptides to be retained and recovered after the dialysis treatment. The small average molecular weight of the Alcalase hydrolyzed samples caused a large portion of the di-, tri-peptides, and single amino acids to be lost into the dialysis buffer. Thus, the repeatability of the mass balance suggests that the dialysis treatment and fractionation were repeatable, which will be further discussed later during subsequent sample characterization.

3.2.5. *IRI activities of the IMAC fractionated and further processed samples*

The newly fractionated trial 1 and 2 IMAC fractions, IMAC combination samples, and hydrolysate dialysis samples were then evaluated for their IRI activities in the splat assay. As shown in Table 4, the hydrolysates and dialyzed hydrolysates before IMAC treatment showed no IRI, displaying average crystal diameters larger than PEG. Paralleling our screening trial, all the IMAC fractionated pulse hydrolysates showed enhanced IRI activity after fractionation, with a reduction of ice crystal Feret's diameter as large as ~50%. In contrast to our hypothesis, the B fractions possessed potent IRI activity in the case of the B Alc chickpea trial 1 and 2. Interestingly, the B fraction IRI is seemingly larger than the UB fractions except for the UB and B Alc pea trial 1 fractions, but this was found not to be statistically significant when compared to the IRI activities of the UB fractions. The IRI activities of the fractionated

Table 4
Molecular weight, Na^+ concentration, and IRI activities of the selected trial 1 and 2 pulse protein Ni^{2+} IMAC fractions.

Sample	Fraction	MW (kDa)		Na^+ Conc. (mM)		FD (%PEG)	
		T1	T2	T1	T2	T1	T2
Alc Chickpea	Hydrolysate	3.2	ND	14	ND	106.0 ± 0.1^{a}	ND
	Hydrolysate Dialysis	13.0	ND	13	ND	106.9 ± 3.0^{a}	ND
	Combo	5.0	ND	56	ND	52.6 ± 0.2^{g}	ND
	Unbound	2.3	1.3	67	83	66.2 ± 2.2^{defg}	75.9 ± 5.0^{cdef}
	Bound	10.0	13.9	48	87	57.5 ± 4.4^{efg}	54.6 ± 0.5^{fg}
Alc Pea	Hydrolysate	1.3	ND	36	ND	105.0 ± 3.0^{a}	ND
	Hydrolysate Dialysis	5.6	ND	13	ND	103.3 ± 4.8^{ab}	ND
	Combo	3.2	ND	45	ND	56.4 ± 3.6^{efg}	ND
	Unbound	3.5	1.2	52	65	59.1 ± 2.9^{efg}	76.8 ± 1.3^{cdef}
	Bound	8.0	5.1	43	57	82.8 ± 2.7^{bcd}	70.7 ± 3.3^{cdefg}
Try Soy	Hydrolysate	28.6	ND	18	ND	103.7 ± 0.5^{ab}	ND
	Hydrolysate Dialysis	31.0	ND	22	ND	102.6 ± 2.5^{ab}	ND
	Combo	28.6	ND	49	ND	77.4 ± 12.3^{cde}	ND
	Unbound	25.0	22.0	65	74	72.3 ± 4.6^{cdefg}	89.6 ± 0.7^{abc}
	Bound	38.3	39.8	61	52	65.5 ± 1.5^{defg}	59.5 ± 2.8^{efg}

T1 represents trial 1, T2 represents trial 2 of the replicate IMAC separation. The Feret diameter value is the percent ice crystal size relative to the PEG control at 2%. Thus, 100% would indicate that the ice crystal size induced by the sample was the same size as the IRI inactive PEG control. The standard deviation is the variation of crystal size (%) between duplicate splat assay measurements. All Na + measurements and Avg MW measurements were made in duplicate. ND incidicates not done.
[a]Means followed by different letter(s) within the same column are significantly different from each other ($P < 0.05$, $n = 2$).

peptides varied slightly between the trials and is likely attributed to probable differences in peptide compositions collected within the fractions. Also in Table 4, the unbound and bound fractions showed higher IRI activity as compared to the hydrolysates that did not undergo IMAC separation. It is possible that the IMAC fractionation altered the structure of the peptide mixtures and their ability to cooperatively occupy the ice water interface that results in the inhibition of ice recrystallization. Thus, we believe that the IMAC fractionation altered the peptides' ability to favorably orient themselves at the ice-water interface resulting in IRI. (Ollis, Wang, & Dia, 2024). Many small differences in the different peptide fraction molecular characteristics between the trials may induce slight changes in IRI as multiple mechanisms attributed to IRI have been identified in literature corresponding to a wide number of molecular characteristics.

Remarkably, the "combination sample" created by combining the UB and B peptide fractions after fractionation, displayed potent IRI activity typically inducing mean crystal diameter values between the B and UB fractions. IRI activity has a close relationship with an array of molecular characteristics, including amphiphilicity mediated by amino acid R-groups, protein structure, molecular weight, solvent ionic strength, etc. (Biggs et al., 2019). Thus, this newly realized IRI activity was hypothesized to be the result of multiple molecular characteristics working in tandem to promote the IRI activity of the samples. Thus, we investigated the molecular characteristics of these samples to deduce the source of these new IRI activities, and particularly, why IMAC treatment induced IRI activity.

3.3. Characterization of pulse hydrolysates Ni^{2+} IMAC fractions' physicochemical properties related to IRI

3.3.1. Sodium ion quantification of the Ni^{2+} IMAC samples

To determine the source of the fractionated samples' and combination samples' IRI activity, the residual sodium ion content was characterized. Standard fractionation of proteins in IMAC requires buffers with large amounts of salt to screen potential electrostatic interactions between amino acids and column components (Gutiérrez et al., 2007). While it is necessary to create a selective coordination-complex-based binding affinity, high and non-uniform concentrations of salt can interfere with IRI assessment in the splat assay (Surís-Valls & Voets, 2019a). Thus, to remove excess salt from the IMAC fractions, dialysis was performed. The remaining sodium ion concentration after dialysis can be seen in Table 4. Although the identical dialysis method was repeated for both trials 1 and 2, the endpoint sodium ion measurements displayed random differences in final sodium ion concentrations. While the source of this difference in dialysis efficacy is unknown, it may be affected by multiple factors including differences in water temperature, initial sodium quantity, total volume of the IMAC fraction after partial lyophilization before dialysis, membrane tightness, and sodium ion binding potential of different peptides present in the different fractions and trials (McPhie, 1971). The combination samples showed sodium levels similar to trials 1 and 2 of the fractionated samples, indicating that the combination of the samples may not have affected the end-point sodium content greatly. The hydrolysate sample controls (no fractionation) had minimal sodium ions resulting from neutralization reactions during the adjustment of pH during the hydrolysis step. Finally, the whole dialysis samples displayed the lowest concentration of sodium resulting from the low initial concentration of salt in the sample and subsequent dialysis treatment. The retention of sodium ions after the 4-day dialysis in all of the protein samples is likely due to the protein's high affinity to bind and interact with sodium, potentially equilibrating at a low concentration of sodium ions due to the presence of the peptide mixtures (Zhang, 2012). Hence, these retained salts present after extensive dialysis may indicate that the salts were bound to the peptide mixtures playing a potential role in stabilizing and inducing structure for these mixtures, as the interaction affinities of salts and the charged amino acid groups may be more favorable than the osmotic gradient present during dialysis, leading to the higher end point recoveries (Zhang, 2012). Despite the differing amounts of salts possessed by the IMAC samples evaluated, statistically, salt concentration was found to have no correlation with IRI.

3.3.2. Average molecular weight quantification of the Ni^{2+} IMAC samples

Next, the average MW of the trial 1 and 2 IMAC fractions were quantified, seen in Table 4. Comparing the two trials, similar average MW values were obtained for all the fractions. Comparing the UB and B fraction MW within trials, the average MW of the peptides in the B fraction were consistently larger than the UB fraction suggesting that histidine and cysteine were present in the sequence of larger peptides, or that MW compatibility allowing multi-point attachment of amino acids to immobilized metal ions allowed these peptides to be retained and enriched in this fraction (Gutiérrez et al., 2007). According to previous studies, peptide fractions with molecular weights between 2 and 5 kDa displayed the highest IRI activity as observed in peptides created from fish gelatin (Damodaran & Wang, 2017). Another study found that collagen hydrolysates with molecular weights between 0.7 and 1.4 kDa displayed the highest IRI activity, demonstrating how generally,

peptides ranging from 0.5 kDa to 5 kDa possess the best ability to inhibit the recrystallization of ice (Wang, Agyare, & Damodaran, 2009). Interestingly, we found no correlation between MW and IRI activity, instead observing that all of the peptide fractions that passed through the IMAC column with average molecular weights ranging from 2 kDa to 38 kDa, displayed IRI activity, contrasting the trends observed from these previous studies. Close similarities in average MW between the two trials along with the mass balance of the fractions and amino acid composition, discussed next, indicate high repeatability in fractionation of these peptides into the B and UB fractions. Regardless, correlation analysis found no relationship between MW and IRI activity, prompting us to investigate other molecular characteristics of the fractions.

3.3.3. Amino acid composition of the Ni^{2+} IMAC samples

Next, the amino acid compositions of the UB and B fractions were characterized to evaluate the relationship between amino acid composition and IRI activity, as shown in Supplementary Fig. 1. Unfortunately, tryptophan's instability during acid hydrolysis did not allow quantification of this residue in the HPLC assay. IMAC fractionation of peptides of is largely based on three key amino acids, His, Cys, and Trp. The most important amino acid in IMAC binding is His, followed by Cys and then finally Trp (Porath, 1992). Because we saw clear enrichment of His and Cys by IMAC fractionation and because Trp cannot be quantified by our current amino acid HPLC-based method, it can be indicated that our IMAC fraction was carried out successfully as the two strongest determinants of fractionation (His and Cys) were successfully enriched in the bound fraction. Seen in Supplementary Fig. 1, the abundance of histidine and cysteine residues displayed clear enrichment of these amino acids into the B fractions with no or trace quantities present in the UB fractions. Aside from the enrichment of these key amino acid residues responsible for the separation of the peptides into the UB and B fractions, the composition of the other amino acid residues in the IMAC fractions and between trials showed close similarities. Furthermore, the categorization of amino acids by their structural features including neutral nonpolar, neutral polar, basic, and acidic amino acid residue categories displayed similar compositions between the UB and B fractions and between trials. Thus, this data supports the successful implementation of IMAC through the enrichment of peptides containing cysteine and histidine into the B fraction, and together with the mass balance and average MW data shows that the IMAC treatment performed a successful and consistent separation between the trials. As discussed previously, the amino acid composition of IRI active hydrolyzed collagen lacked tryptophan, cysteine, and significant quantities of histidine, which were thought to contribute to these peptides IRI abilities (Cao et al., 2020). In our study, we found that regardless of histidine and cysteine, all peptide fractions that were separated via IMAC showed IRI activity in comparison to their non fractionated counterparts. Though the IMAC treatment properly fractionated the pulse peptides into UB and B fractions, no statistical correlation was found between the IMAC fractions' amino acid composition and their IRI activities, in contrast to our hypothesis.

3.3.4. Secondary structure quantification of the Ni^{2+} IMAC samples

To further characterize the IMAC fractions and evaluate the relationship between their molecular structure features and IRI activity, the secondary structures of the IMAC fractionated samples, whole dialysis samples, and starting pulse hydrolysates were quantified by Raman Spectroscopy. As shown in Fig. 1, resulting from the hydrolysis treatment that creates a diverse composition of peptides with differing amino acid residues and chain lengths, the Alcalase and trypsin hydrolysate samples showed differences in their secondary structures. Furthermore, the Alcalase chickpea and pea hydrolysate samples showed close similarities in their secondary structure makeup, likely due to their similarities in MW and similar sources of storage proteins (Barac et al., 2010; Chang, Alli, Konishi, & Ziomek, 2011). Additionally, the whole dialysis samples' secondary structure composition is distinct from that of the starting hydrolysates due to the dialysis treatment removing peptides under 3.5 kDa. The combination samples and individual UB and B IMAC fractions seem to show less of a trend pertaining to their secondary structure makeup. Though the UB and B try soy samples and UB and B Alc chickpea samples show some similarities in their beta-sheet percentages displaying a lower abundance of beta-sheet for the UB fraction relative to the B samples. According to Surís-Valls and Voets (2019b), high percentages of α-helical structures, β-strands (including β-solenoids) and polyproline II helices are of importance for the IRI activity of natural anti-freeze proteins. Though our peptide mixtures showed relatively uniform promotion of IRI after IMAC fractionation, no clear secondary structural trend was observed, contrasting the various natural

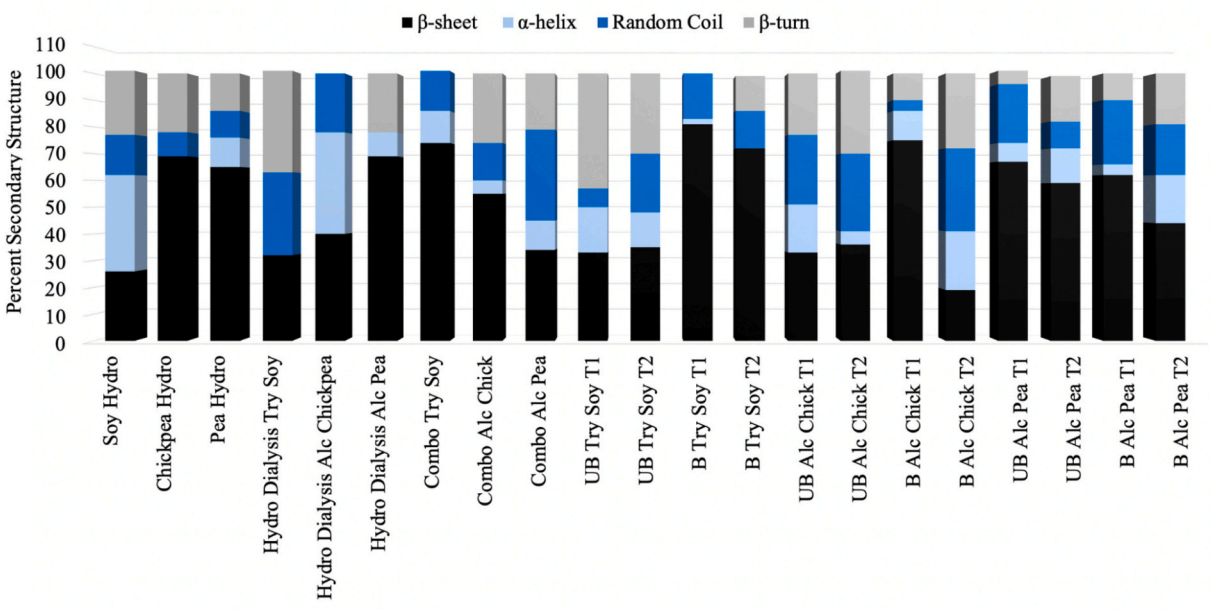

Fig. 1. Secondary structure profiles of the selected Ni 2+ IMAC fractions and hydrolysate samples. T1 represents trial 1, T2 represents trial 2 of the replicate IMAC treatments. Secondary structure measurements were made in duplicate.

AFPs structural similarities. This difference may be attributed to the natural AFPs mechanism of action often producing IRI through ice binding, whereas IRI activity from peptides typically do not show specific ice binding abilities contingent on their structure and amino acid resiude placements (Surís-Valls & Voets, 2019b). It should also be noted that the amount of residual salt discussed previously may affect the presentation and type of secondary structure, as cations' interaction with the peptide bond and amino acid side chains alongside competitive binding with water molecules and intrachain H-bonds may destabilize secondary structure, potentially burying any trends induced by the IMAC treatment (Okur et al., 2017). Considering this salt effect that may hide secondary structural trends with IRI activity, it is unsurprising that statistically the secondary structure profiles of the peptide chains showed no relationship with their respective IRI activities.

3.3.5. *Alc chickpea splat assay under different buffer conditions*

To further elucidate the IRI activities of the IMAC fractionated pulse proteins and combination samples, additional splat assay model systems were created using several dispersing mediums containing different salts and metal ions. These characterizations were performed to evaluate the possibility of metal ion transfer from the IMAC column into the collected peptide mixtures, potentially chelating the peptides and creating aggregates that may be responsible for their IRI (Porath, 1992; Rotilio, 1980). Further, additional salts were also evaluated in the splat assay dispersing mediums to evaluate if there was a critical salt concentration or pH condition needed to induce IRI across the IMAC treated samples, as previously, the splat assay dispersing medium has been reported to play a role in altering IRI and ice nucleation (Surís-Valls & Voets, 2019a). Thus, using the 4% (*w/v*) Alc chickpea hydrolysate as a model "IRI inactive" control, dispersing medium conditions were altered to try to induce IRI activity. Interestingly, as shown in Fig. 2, none of the solvent or pH conditions promoted the IRI of the Alcalase hydrolysate sample. Unexpectedly, a trend of increasing ice crystal size with increasing sodium concentration was observed as this trend has been reported previously (Delesky & Srubar 3rd., 2022). Thus, the sodium concentration retained by the peptides during dialysis or pH differences stemming from the IMAC fractionation could not have promoted IRI activity, suggesting that the IRI activity of the IMAC samples was mediated through their individual molecular characteristics.

To further explore the relationship between the dispersing medium conditions experienced by the IMAC fractionated samples and their IRI activities, we performed the splat assay with different concentrations of the IMAC elution and equilibration buffers to evaluate the effect on the ice crystal size induced by the Alc chickpea hydrolysate. Additionally, we diluted the IMAC buffers down to concentrations mirroring the IMAC fraction's sodium ion content recorded in Table 4, to more closely represent the realistic solvent environments the hydrolysates were evaluated in, additionally matching the analyte concentration to 2 and 4%. As seen in Fig. 3, the presence of both sodium phosphate and sodium chloride from the IMAC buffers did not induce IRI for the hydrolysate in a multitude of IMAC buffer concentrations.

Finally, to investigate the possible metal ion transfer events that could potentially induce IRI activity, we evaluated the Alc chickpea hydrolysate with the addition of two structure-forming metal ions, nickel and calcium known to bind proteins that may potentially induce IRI as has been reported for calcium (Delesky, Thomas, Charrier, Cameron, & Srubar 3rd., 2021). Similar to results obtained with the IMAC buffers seen in Fig. 3, the addition of the metal ions did not induce IRI, suggesting that possible contamination of metal ions during IMAC was not the source of the IRI viewed in nickel fractionated IMAC hydrolysates. This conclusion was also supported by the particle size distribution of the Ni^{2+} IMAC try soy samples that showed little differences between the hydrolysate sample, combination samples, and IMAC fraction particle size distributions, indicating that aggregation mediated through metal ion-protein interactions was not responsible for the IMAC fractions' IRI activities (Supplementary Fig. 3).

4. Conclusions and perspectives

We have fully demonstrated for the first time, the ability of Ni^{2+} IMAC to fractionate protein hydrolysates by their amino acid compositions to create peptide mixtures capable of inhibiting the recrystallization of ice from widely available food materials. While Ni^{2+} IMAC treatment has shown clear and significant promotion of IRI activities from inactive pulse source materials, the structure-function relationship of the peptide mixtures and their IRI activities could not be definitively stated. Our hypothesis that IMAC fractionation will result in the production of IRI active peptide mixtures was proven. On the other hand, the hypothesis that B fraction lacking His and Cys will not possess IRI activity was not observed as both B and UB fractions from IMAC were IRI active. While none of the individual characterizations showed a relationship with IRI activity, the combination of these characteristics working in tandem could potentially be the source of this IRI activity. It must also be considered that the quantification techniques used to try to describe the relationship between molecular characteristics and IRI, measured here at ambient temperatures, may be insufficient to describe

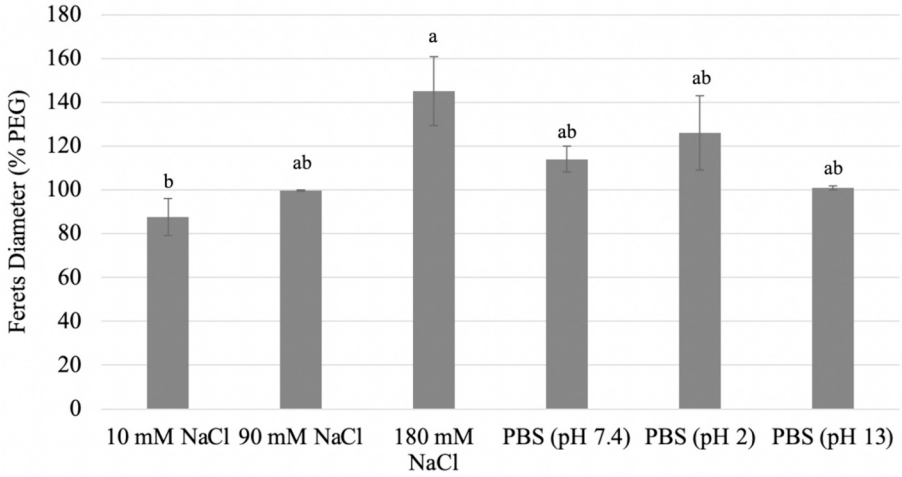

Fig. 2. Alcalase Chickpea hydrolysate IRI in different dispersing mediums varying salt concentration and pH. The Feret diameter percentage is relative to the ice crystal size induced by 4% PEG in the same solvent as the Alc chickpea hydrolysate for each respective sample. The standard deviation is the variation of crystal size (%) between duplicate splat assay measurements. [a]Means followed by different letter(s) within the same column are significantly different from each other ($P < 0.05$, $n = 2$).

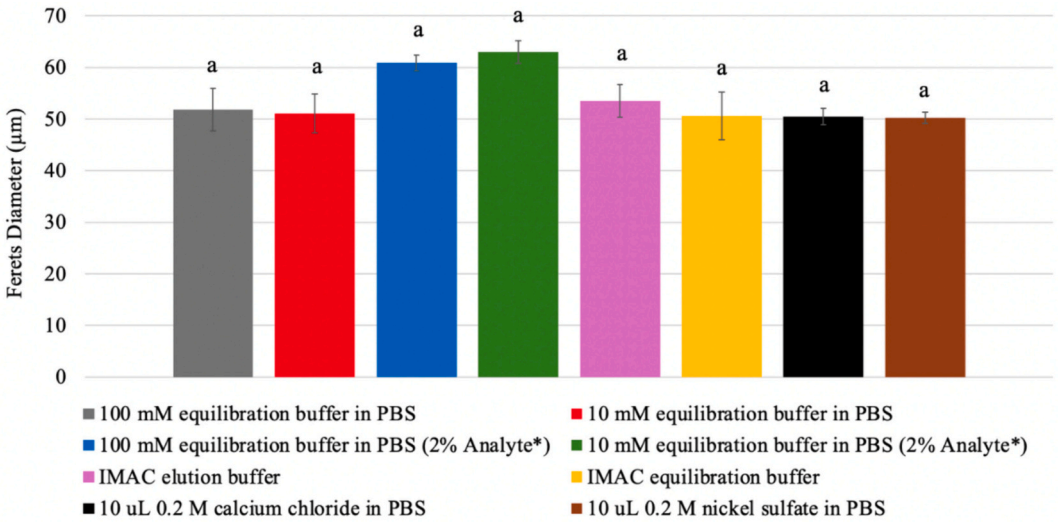

Fig. 3. Alcalase chickpea hydrolysate IRI in different dispersing mediums containing the IMAC buffers and metal ions. 4% PEG in 1× PBS induced a mean ice crystal diameter of 43.8 ± 0.7 µm. The standard deviation is the variation of crystal size (µm) between duplicate splat assay measurements. [a]Means followed by different letter(s) within the same column are significantly different from each other ($P < 0.05$, $n = 2$).

how the vastly different microenvironment of the ice-water interface and low temperatures affect these dynamic molecules, including peptide folding, H-bonding and their potential for cooperative effects at the interface under these conditions. Regardless, the impact of our novel Ni^{2+} IMAC treatment of pulse hydrolysates may provide a new method of producing IRI active molecules for potential use as preservation agents for foods and biomedical materials. Future work should include the characterization of additional molecular characteristics, under relevant conditions (ice-water interface, below the freezing point) and more advanced statistical modeling that may be able to elucidate the source of the peptide fractions IRI. Further, investigation of differing protein hydrolysates outside of pulses and the use of differing immobilized metal ions should be conducted to determine the ability of IMAC to produce IRI active peptides from diverse sources of proteins, and further evaluate the effect of the immobilized metal ions' role in inducing these molecules IRI activities.

Funding

This work was supported by the National Science Foundation through funding (award number 2103558) and Hatch/Multi-state project (accession number: 1023982).

CRediT authorship contribution statement

Joshua Saad: Writing – original draft, Visualization, Validation, Methodology, Investigation, Formal analysis, Data curation, Conceptualization. **Murillo Longo Martins:** Writing – review & editing, Methodology, Formal analysis, Data curation. **Vermont Dia:** Writing – review & editing, Validation, Supervision, Resources, Project administration, Methodology, Funding acquisition, Conceptualization. **Toni Wang:** Writing – review & editing, Supervision, Resources, Project administration, Methodology, Funding acquisition, Conceptualization.

Declaration of competing interest

The authors declare that they have no conflict of interests.

Data availability

Data will be made available on request.

Acknowledgement

The authors of this article would like to thank Dr. Alexei Sokolov's lab for providing us access to the Raman spectrometer and for sharing additional resources used to complete this work.

Appendix A. Supplementary data

Supplementary data to this article can be found online at https://doi.org/10.1016/j.foodchem.2024.140574.

References

Akhlaghi, Y., Ghaffari, S., Attar, H., & Alamir Hoor, A. (2015). A rapid hydrolysis method and DABS-Cl derivatization for complete amino acid analysis of octreotide acetate by reversed phase HPLC. *Amino Acids, 47*(11), 2255–2263. https://doi.org/10.1007/s00726-015-1999-9

Barac, M., Cabrilo, S., Pesic, M., Stanojevic, S., Zilic, S., Macej, O., & Ristic, N. (2010). Profile and functional properties of seed proteins from six pea (*Pisum sativum*) genotypes. *International Journal of Molecular Sciences, 11*(12), 4973–4990. https://doi.org/10.3390/ijms11124973

Bhattacharya, M., Hota, A., Kar, A., Sankar Chini, D., Chandra Malick, R., Chandra Patra, B., & Kumar Das, B. (2018). In silico structural and functional modelling of antifreeze protein (AFP) sequences of ocean pout (*Zoarces americanus*, Bloch & Schneider 1801). *Journal of Genetic Engineering and Biotechnology, 16*(2), 721–730. https://doi.org/10.1016/j.jgeb.2018.08.004

Biggs, C. I., Stubbs, C., Graham, B., Fayter, A. E. R., Hasan, M., & Gibson, M. I. (2019). Mimicking the ice recrystallization activity of biological antifreezes. When is a new polymer "active"? *Macromolecular Bioscience, 19*(7), Article e1900082. https://doi.org/10.1002/mabi.201900082

Bradley, M. (n.d.). Curve fitting in Raman and IR spectroscopy: Basic theory of line shapes and applications. https://assets.thermofisher.com/TFS-Assets/CAD/Application-Notes/AN50733_E.pdf.

Cao, H., Zheng, X., Liu, H., Yuan, M., Ye, T., Wu, X., Yin, F., Li, Y., Yu, J., & Xu, F. (2020). Cryo-protective effect of ice-binding peptides derived from collagen hydrolysates on the frozen dough and its ice-binding mechanisms. *LWT, 131*, Article 109678. https://doi.org/10.1016/j.lwt.2020.109678

Cao, S., Cai, J., Wang, X., Zhou, K., Liu, L., He, L., Qi, X., & Yang, H. (2023). Cryoprotective effect of collagen hydrolysates from squid skin on frozen shrimp and characterizations of its antifreeze peptides. *LWT, 174*, Article 114443. https://doi.org/10.1016/j.lwt.2023.114443

Chang, Y.-W., Alli, I., Konishi, Y., & Ziomek, E. (2011). Characterization of protein fractions from chickpea (*Cicer arietinum* L.) and oat (*Avena sativa* L.) seeds using proteomic techniques. *Food Research International, 44*(9), 3094–3104. https://doi.org/10.1016/j.foodres.2011.08.001

Damodaran, S., & Wang, S. (2017). Ice crystal growth inhibition by peptides from fish gelatin hydrolysate. *Food Hydrocolloids, 70*, 46–56. https://doi.org/10.1016/j.foodhyd.2017.03.029

Delesky, E. A., & Srubar, W. V., 3rd. (2022). Ice-binding proteins and bioinspired synthetic mimics in non-physiological environments. *iScience, 25*(5), Article 104286. https://doi.org/10.1016/j.isci.2022.104286

Delesky, E. A., Thomas, P. E., Charrier, M., Cameron, J. C., & Srubar, W. V., 3rd. (2021). Effect of pH on the activity of ice-binding protein from *Marinomonas primoryensis*. *Extremophiles, 25*(1), 1–13. https://doi.org/10.1007/s00792-020-01206-9

Fomich, M., Día, V. P., Premadasa, U. I., Doughty, B., Krishnan, H. B., & Wang, T. (2023). Ice recrystallization inhibition activity of soy protein hydrolysates. *Journal of Agricultural and Food Chemistry, 71*(30), 11587–11598. https://doi.org/10.1021/acs.jafc.2c08701

Gutiérrez, R., Martín del Valle, E. M., & Galán, M. A. (2007). Immobilized metal-ion affinity chromatography: Status and trends. *Separation and Purification Reviews, 36*(1), 71–111. https://doi.org/10.1080/15422110601166007

Holmes, L. D., & Schiller, M. R. (1997). Immobilized Iron(III) metal affinity chromatography for the separation of phosphorylated macromolecules: Ligands and applications. *Journal of Liquid Chromatography & Related Technologies, 20*(1), 123–142. https://doi.org/10.1080/10826079708010641

Knight, C. A., Hallett, J., & DeVries, A. L. (1988). Solute effects on ice recrystallization: An assessment technique. *Cryobiology, 25*(1), 55–60. https://doi.org/10.1016/0011-2240(88)90020-x

Li, T., Zhao, Y., Zhong, Q., & Wu, T. (2019). Inhibiting ice recrystallization by nanocelluloses. *Biomacromolecules, 20*(4), 1667–1674. https://doi.org/10.1021/acs.biomac.9b00027

Lin, S., Hu, X., Li, L., Yang, X., Chen, S., Wu, Y., & Yang, S. (2021). Preparation, purification and identification of iron-chelating peptides derived from tilapia (*Oreochromis niloticus*) skin collagen and characterization of the peptide-iron complexes. *LWT, 149*, Article 111796. https://doi.org/10.1016/j.lwt.2021.111796

Lingg, N., Öhlknecht, C., Fischer, A., Mozgovicz, M., Scharl, T., Oostenbrink, C., & Jungbauer, A. (2020). Proteomics analysis of host cell proteins after immobilized metal affinity chromatography: Influence of ligand and metal ions. *Journal of Chromatography. A, 1633*, Article 461649. https://doi.org/10.1016/j.chroma.2020.461649

Lv, Y., Bao, X., Liu, H., Ren, J., & Guo, S. (2013). Purification and characterization of calcium-binding soybean protein hydrolysates by Ca2+/Fe3+ immobilized metal affinity chromatography (IMAC). *Food Chemistry, 141*(3), 1645–1650. https://doi.org/10.1016/j.foodchem.2013.04.113

McPhie, P. (1971). [4] Dialysis. In *, Vol. 22. Methods in enzymology* (pp. 23–32). Academic Press. https://doi.org/10.1016/0076-6879(71)22006-1.

Okur, H. I., Hladílková, J., Rembert, K. B., Cho, Y., Heyda, J., Dzubiella, J., … Jungwirth, P. (2017). Beyond the Hofmeister series: Ion-specific effects on proteins and their biological functions. *The Journal of Physical Chemistry B, 121*(9), 1997–2014. https://doi.org/10.1021/acs.jpcb.6b10797

Ollis, A., Wang, T., & Dia, V. P. (2024). Hemp protein hydrolysates' ability to inhibit ice recrystallization is influenced by the dispersing medium and succinylation. *Food Hydrocolloids, 147*(A), Article 109375. https://doi.org/10.1016/j.foodhyd.2023.109375

Porath, J. (1988). IMAC—Immobilized metal ion affinity based chromatography. *TrAC Trends in Analytical Chemistry, 7*(7), 254–259. https://doi.org/10.1016/0165-9936(88)85074-X

Porath, J. (1992). Immobilized metal ion affinity chromatography. *Protein Expression and Purification, 3*(4), 263–281. https://doi.org/10.1016/1046-5928(92)90001-D

Rotilio, G. (1980). Interaction of metal ions with proteins: An overview. *Inorganica Chimica Acta, 40*, X49. https://doi.org/10.1016/S0020-1693(00)92105-4

Saad, J., Fomich, M., Día, V. P., & Wang, T. (2023). A novel automated protocol for ice crystal segmentation analysis using Cellpose and Fiji. *Cryobiology, 111*, 1–8. https://doi.org/10.1016/j.cryobiol.2023.02.002

Saad, J. S., & Dia, V. P. (2023). Bromelain hydrolysis modified the functionality, antioxidant, and anti-inflammatory properties of hempseed (*Cannabis sativa* L.) protein isolated at pH 12. *ACS Food Science & Technology, 3*(6), 1049–1056. https://doi.org/10.1021/acsfoodscitech.3c00033

Surís-Valls, R., & Voets, I. K. (2019a). The impact of salts on the ice recrystallization inhibition activity of antifreeze (Glyco)proteins. *Biomolecules, 9*(8). https://doi.org/10.3390/biom9080347

Surís-Valls, R., & Voets, I. K. (2019b). Peptidic antifreeze materials: Prospects and challenges. *International Journal of Molecular Sciences, 20*(20). https://doi.org/10.3390/ijms20205149

Tacias-Pascacio, V. G., Morellon-Sterling, R., Siar, E.-H., Tavano, O., Berenguer-Murcia, Á., & Fernandez-Lafuente, R. (2020). Use of Alcalase in the production of bioactive peptides: A review. *International Journal of Biological Macromolecules, 165*, 2143–2196. https://doi.org/10.1016/j.ijbiomac.2020.10.060

Tian, Y., Zhu, Z., & Sun, D.-W. (2020). Naturally sourced biosubstances for regulating freezing points in food researches: Fundamentals, current applications and future trends. *Trends in Food Science & Technology, 95*, 131–140. https://doi.org/10.1016/j.tifs.2019.11.009

Vajda, T., & Szabó, T. (1976). Specificity of trypsin and alpha-chymotrypsin towards neutral substrates. *Acta Biochimica et Biophysica; Academiae Scientiarum Hungaricae, 11*(4), 287–294.

Voets, I. K. (2017). From ice-binding proteins to bio-inspired antifreeze materials [10.1039/C6SM02867E]. *Soft Matter, 13*(28), 4808–4823. https://doi.org/10.1039/C6SM02867E

Wang, S., Agyare, K., & Damodaran, S. (2009). Optimisation of hydrolysis conditions and fractionation of peptide cryoprotectants from gelatin hydrolysate. *Food Chemistry, 115*(2), 620–630. https://doi.org/10.1016/j.foodchem.2008.12.079

Wang, S., Zhao, J., Chen, L., Zhou, Y., & Wu, J. (2014). Preparation, isolation, and hypothermia protection activity of antifreeze peptides from shark skin collagen. *LWT, 55*(1), 210–217. https://doi.org/10.1016/j.lwt.2013.07.019

Warren, M. T., Galpin, I., Bachtiger, F., Gibson, M. I., & Sosso, G. C. (2022). Ice recrystallization inhibition by amino acids: The curious case of alpha- and Beta-alanine. *The Journal of Physical Chemistry Letters, 13*(9), 2237–2244. https://doi.org/10.1021/acs.jpclett.1c04080

Zhang, G., Zhu, C., Walayat, N., Nawaz, A., Ding, Y., & Liu, J. (2023). Recent development in evaluation methods, influencing factors and control measures for freeze denaturation of food protein. *Critical Reviews in Food Science and Nutrition, 63*(22), 5874–5889. https://doi.org/10.1080/10408398.2022.2025534

Zhang, J. (2012). Protein-protein interactions in salt solutions. *Protein-protein Interactions-computational and Experimental Tools, 6*, 359–376. https://doi.org/10.5772/38056

Zhang, Y., Wang, W., Liu, Y., Liu, X., Wang, H., & Zhang, H. (2022). Cryoprotective effect of wheat gluten enzymatic hydrolysate on fermentation properties of frozen dough. *Journal of Cereal Science, 104*, Article 103423. https://doi.org/10.1016/j.jcs.2022.103423